

Target Parameter Estimation in Frequency Diverse Array Radar using Sparse Reconstruction Algorithms



By

Ayesha Ansari

MSEE-25

Supervisor

Asst. Prof. Hussain Ali, PhD

Department of Electrical Engineering

A thesis submitted in partial fulfillment of the requirements for the degree of
Masters in Electrical Engineering

In

Military College of Signals,

National University of Sciences and Technology (NUST),

Islamabad, Pakistan.

(March 2023)


THESIS ACCEPTANCE CERTIFICATE

Certified that final copy of MS/MPhil thesis written by Ms. NS Ayesha Ansari, Registration No. 00000318572 of Military College of Signals has been vetted by undersigned, found complete in all respect as per NUST Statutes/Regulations, is free of plagiarism, errors and mistakes and is accepted as partial, fulfillment for award of MS/MPhil degree. It is further certified that necessary amendments as pointed out by GEC members of the student have been also incorporated in the said thesis.

Signature:  **Dr. Hussain Ali**
Assistant Professor (Dept of EE)
Military College of Signals (NUST)

Name of Supervisor Asst Prof Hussain Ali, PhD

Date: _____

Signature (HoD):  **Brig HoD**
Dept of Elec Engg
Military College of Signals (NUST)
(NUST Campus)

Date: _____

Signature (Dean): 

Date: 18/7/23

Brig Dean, MCS (NUST)
(Asif Masood, Phd)

Dedication

This study is entirely dedicated to my dear parents, who have been my source of motivation and strength when I felt like giving up, and who consistently offer their moral, spiritual, emotional, and financial support.

Certificate of Originality

I hereby declare that this submission is my own work and to the best of my knowledge it contains no materials previously published or written by another person, nor material which to a substantial extent has been accepted for the award of any degree or diploma at Department of Electrical Engineering at Military College of Signals or at any other educational institute, except where due acknowledgement has been made in the thesis. Any contribution made to the research by others, with whom I have worked at Military College of Signals or elsewhere, is explicitly acknowledged in the thesis. I also declare that the intellectual content of this thesis is the product of my own work, except for the assistance from others in the project's design and conception or in style, presentation and linguistics which has been acknowledged.

Author Name: Ayesha Ansari

Signature: _____

Acknowledgments

Glory be to Allah (S.W.A), the Creator, the Sustainer of the Universe. Who only has the power to honour whom He please, and to abase whom He please. Verily no one can do anything without His will. From the day, I came to NUST till the day of my departure, He was the only one Who blessed me and opened ways for me, and showed me the path of success. There is nothing which can payback for His bounties throughout my research period to complete it successfully.

Ayesha Ansari

Contents

1	Introduction	1
1.1	The Evolution of Radar Through History.	1
1.2	Fundamental Radar Functions	2
1.3	Types of Radar	3
1.3.1	Monostatic Radar	3
1.3.2	Frequency Diverse Array Radar	3
1.4	Application of FDA-Radar	5
1.5	FDA MIMO Radar	5
1.6	Sparse Reconstruction	7
1.7	Sparse reconstruction applications	8
1.8	MUSIC Algorithm	9
1.9	Problem Statement	9
1.10	Summary Of Contributions	10
1.11	Thesis Arrangement	10
2	Comprehensive Review of the Literature	11
2.1	Frequency Diverse Array Radar	11
2.2	Frequency Diverse Array MIMO Radars	18
2.3	Sparse Reconstruction	25

3	Sparse Reconstruction Algorithms	29
3.1	Sparse Reconstruction	29
3.2	Reconstruction of Sparse Signal	29
3.3	Nesterov’s Algorithm (NESTA)	30
3.3.1	Algorithm	31
3.4	Results of Simulation	32
3.5	Fast Bayesian Matching Pursuit	33
3.5.1	Algorithm	34
3.6	Results of Simulation	35
3.7	Orthogonal Matching Pursuit	36
3.7.1	Algorithm	37
3.8	Results of Simulation	37
3.9	Simulation Results of Different Algorithms	38
3.10	Conclusion	39
4	Design and Methodology	40
4.1	Applying sparse reconstruction algorithms	43
4.2	Applying MUSIC algorithm	43
4.3	Simulation Results	44
5	Conclusion	47
	References	48
	A First Appendix	

List of Figures

1.1	Basic Principle of Radar.	3
1.2	Concept of Frequency Diverse Array.	5
1.3	Block diagram of MIMO-FDA radar	6
3.1	Reconstruction of Signal	32
3.2	Nesta Algorithm SNR Vs MSE grap	33
3.3	Reconstruction Signal of FBMP Algorithms	35
3.4	SNR Vs MSE graph of FBMP Algorithm	36
3.5	SNR Vs MSE graph of OMP Algorithm	37
3.6	Comparison between different algorithms.	38
4.1	Comparison of different algorithms applied on FDA	45
4.2	Music algorithm applied on FDA	45
4.3	Comparison of different algorithms RMSE of angle versus SNR	46

List of Tables

3.1 Complexity analysis of Algorithms.	39
--	----

Abstract

The frequency diverse array radar has brought a lot of interest due to the periodicity of the beampattern in angle, time, and range. It is possible to transmit energy over the required coverage and angle with only a small variation in frequency, yielding an array factor from the angle, duration, and range. This newer technique, MIMO FDA (which refers to multiple inputs and multiple Output frequency diversity array), was recently invented. It is intended to improve upon FDA radar in various ways. It is a hybrid of MIMO and FDA, and in the interest of estimating the angle and range simultaneously, a minimum frequency increment is employed in the transmitting antennas, which are positioned near each other. This is done so that the system can calculate both simultaneously. This aims to ensure that the measurements are as accurate as possible. The sparse reconstruction techniques used in this thesis are utilized in a MIMO FDA transmitting array. The one multiple signal classification (MUSIC) technique is utilized for joint angle estimation in FDA-MIMO. As the methodology recommends, estimating angles using an FDA MIMO radar is accomplished by employing sparsity enforced reconstruction technique. When applied to FDA MIMO radar, numerical findings indicate that the FBMP algorithm provides an outstanding Mean Squared Error versus Signal to Noise Ratio performance compared to other algorithms.

CHAPTER 1

Introduction

1.1 The Evolution of Radar Through History.

Radar technology and theory is a vastly advancing field and work has been done in its architecture, concept and different challenges have been updated continuously from time to time in new radar systems. Although "Radio Detection and Ranging" is where the word "Radar" originally came from, with time, it has transformed into a regularly used noun in English speech. It is recognized by a large number of people [1]. Heinrich Hertz, a German physicist, first proved wave reflection in a series of tests in 1885, which is when radar technology first became a reality. Another German physicist, Christian Hulsmeyer, created a monostatic radar device in 1904 that could detect ships. But, at the time of his discovery, the importance of what he had found was not comprehended. In 1922, S. G. Marconi, the man who is credited with inventing the wireless radio, made the observation that the radio may be used to identify targets. L. C. Young and A. H. Taylor of the United States Naval Research Laboratory demonstrated that it was possible to locate ships using radar in the same year (NRL). Hyland made the discovery that radar may be used to identify airplanes in the year 1930. In addition, the initial continuous wave (CW) radar was developed in 1934 and put into operation the same year. Many nations developed and disseminated radar technology independently of one another during World War II, including the USA, UK, the Soviet

Union, France, Germany, Italy, the Netherlands even Japan too [1] [2]. With the conclusion of World War Two, there was surge in the development of radar, which spawned a plethora of new technologies and system modifications; included in this is the result of coherency, as well as the imaging capabilities of synthetic aperture radar (SAR), and the use of pulse compressing in the 1950s, the inclusion of sophisticated antenna structures such as phased arrays or MIMO designs, in addition to ultrawideband radar applications. [3] [4] [5] [6]. Towards the end of the World War second many people had come to understand the usefulness of radar as well as the benefits of microwave frequencies and pulsed waveforms [1]. In the modern world, radar is used for a wide range of operations, include law enforcement, traffic safety, military activities, remote sensing, and space vehicles. Measurement of both distance and speed has been accomplished with the use of radar in a wide range of commercial and industrial contexts, as well as, with caution, to identify the physical characteristics of an interest system.

1.2 Fundamental Radar Functions

Radar is used for environmental sensing as well as the detection and localization of objects like spacecraft, vehicles, ships, and people [2]. In order to identify the presence of the target, the radar first generates an electromagnetic signal through its antenna, which is then used to receive the reflected signal from the target. Modern applications frequently use monostatic radar, which transmits and receives signals using a single antenna. When a pulse is sent out, the duplexer will flip the antenna to its reception mode. This will allow the radar to wait for the pulse to be sent back to it. The target's proximity may be determined using radar by calculating the amount of time that elapses between the pulses sent out and those received. This is the most essential piece of information that radar can supply. However, other information, such as the velocity, size, and orientation of the target, can also be extracted from the received radar signal.

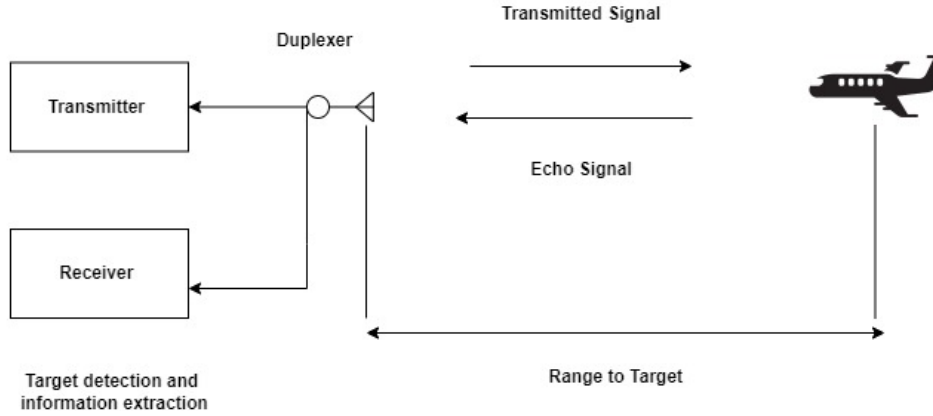


Figure 1.1: Basic Principle of Radar.

1.3 Types of Radar

1.3.1 Monostatic Radar

A monostatic radar is a type of radar system where the transmitter as well as receiver are located at the same location, typically on the same platform or device. In a monostatic radar system, transmit and receive antennas are separate, but they are co-located, typically using a duplexer to isolate the transmit and receive paths. This makes it possible to use the same antenna for transmission and receiving. A lot of applications use monostatic radar systems, comprising surveillance, weather forecasting, and air traffic management. They are relatively simple to design and implement compared to other types of radar systems, and they can provide good performance in many situations. However, they are also subject to interference from clutter and other sources, which can limit their performance in certain environments.

1.3.2 Frequency Diverse Array Radar

FDA idea was introduced by Antonik and Wicks [7] as a technique to perform range dependent beamforming. FDA's unique capabilities are achieved by varying the carrier frequency between its various antennas. In contrast to phased arrays, a frequency increase that is relatively small in contrast to the carrier frequency

is used by elements of FDA. Increase in frequency results in beam pattern. This is based on the range and the angle, which enables range dependent intervention suppression and target localization in [8], [9], and [10], respectively.

Each radiating element in a conventional phased array made up of perfect isotropic radiators produces waveforms identical to the others. If there is no break in the waveforms, they all have the same phase. In this configuration, the antenna beam will be aimed either broadside or perpendicular to the aperture face. On the other hand, this is only valid if the waveforms strike a far field target at a certain angle of θ relative to the broadside direction. The condition mentioned above will not hold true if the phase shift is brought on by a different route length being taken by each constituent.

A traditional phased array differs from the frequency diversity array in terms of the amount of control it provides over beam synthesis. More degrees of freedom are afforded as a result of its generic structure. FDA makes it possible to have a range dependent beamformer and variable beam scanning choices using recent improvements in signal processing technology. In addition, it permits additional modes of radar, such as SAR and moving target indication, which may be used to reduce the effects of point interference caused by phenomena such as multipath.

The traditional phased array creates an electronic beam scan, but the FDA uses a linear phase progression over its aperture. Applying an extra linear frequency shift to the elements causes the generation of a new term, which, when applied to the far field, resulting in an angle of the scan that varies with range. This provides more flexibility in the possibilities for beam scanning and resistance to point interference, such as multipath. The management of space time, frequency, phase, and polarization may benefit from extra degrees of freedom thanks to general implementations.

The novel strategy for joint aperture waveform layouts begins with constructing the frequency diverse array as the initial stage. Transmission of a signal that is a continuous wave from each spatial channel is one of its most fundamental forms. From one channel to the next, a very slightly frequency shift occurs, amounting to

only a few Hertz. Consequently, a beam pattern is produced, resulting in a change in the direction in which the beam is focused. In contrast to the traditional phased array, this transmission considers the sent data's angle, range, and time. In terms of range and duration in the far field, this has a beam that always points in the same direction.

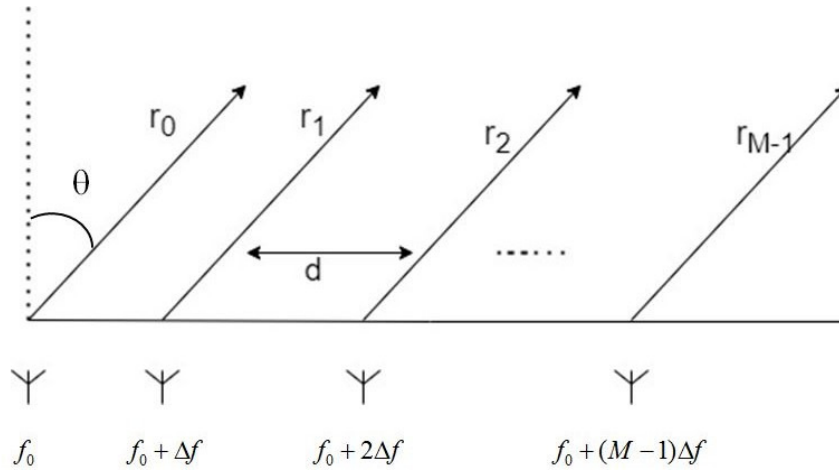


Figure 1.2: Concept of Frequency Diverse Array.

1.4 Application of FDA-Radar

- Target localization
- Target Imaging
- Target Tracking
- Range-dependent beampattern

1.5 FDA MIMO Radar

The FDA is also significantly distinct from MIMO schemes. MIMO has frequently and extensively been used for the purpose of communications applications. This entails many channels, each supplying many independent routes that further lessen

fading effects. Fading is a primary consequence to multipath. Radar is also a contemporary application of MIMO. The MIMO radar concepts are relatively akin to communications applications of MIMO. The MIMO radar ideas also provided numerous unique independent routes attributed to reducing fading caused by changes in the target radar cross section.

MIMO approaches are a salient consideration of contemporary developments; for acquiring closely spaced spatial channels. Large frequency separations between spatial channels are usually opted for, to avoid significant spectral overlap of signals across spatial channels. Moreover, this technique also features a greater degree of spatial channel separation distances; as compared to frequency diverse array. Contrary to that, frequency diverse array utilises slight changes in frequencies between channels. It in turns, leads to a considerable signal overlap. In addition to that, distinct beam properties are also a salient feature of the respective array. In terms of angle, range, and duration, the properties of MIMO FDA radar are different from those of conventional MIMO radar. FDA MIMO radar's enhanced beam features, such as range dependent beamforming and angle independent auto scanning, enable additional capabilities. This is accomplished without the using mechanical beam steering or phase shifters.

It is a mixture of the frequency diverse array and MIMO radar technologies. With this type of radar, antennas close to each other have a slight increase in frequency so that the angle and distance can be calculated simultaneously. Researchers merged FDA radar with MIMO radar to build this new sort of radar. Compared to conventional MIMO radar, this new type offers improved accuracy and range.

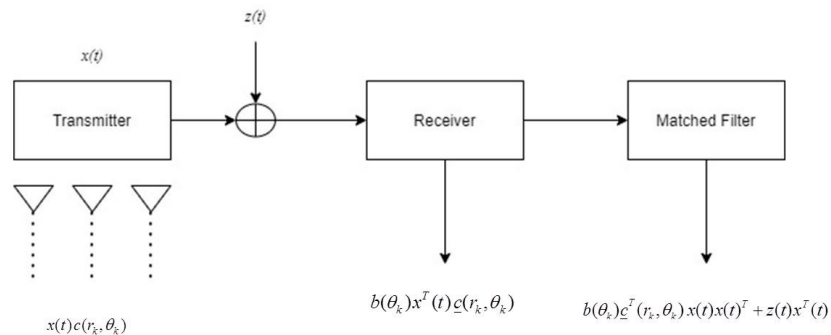


Figure 1.3: Block diagram of MIMO-FDA radar

The above figure shows the transmitting antennas work independently of each other; radiating a distinct arbitrary waveform. Each signal is received by a different antenna. Moreover, due to the distinct nature of the waveforms, a single transmitter can be re-assigned the signals. The transmitted signal, denoted as $x(t)$, is accompanied by a parameter k , which represents the number of uncorrelated targets. The (r_k, θ_k) values represent the range and angle of the k_{th} target respectively. Transmitting side consists of multiple transmitters that generate high frequency signals. These signals are sent to multiple antennas for transmission. As in the receiving section it consists of multiple antennas that receive the reflected signals from the target. Received signals are sent to the receiver section for processing. These signals are amplified, filtered, and demodulated to extract the target information. After that various signal processing operations such as Doppler filtering, pulse compression, and beamforming are done. After that target detection and tracking processes to detect or track the target.

1.6 Sparse Reconstruction

Sparse reconstruction is technique which uses signal sample properties to reconstruct under sampled k spaced data. The target parameters are mainly estimated by creating a model of a sparse signal and reconstructing its spatial spectrum. Many real signals can be considered sparse in some domain, meaning they have a large number of elements that are either equal to or close to zero. A sparse signal is a signal that has a small number of non-zero elements in relation to its dimension. Shannon-Nyquist theorem is used for the reconstruction of signals, and it enables more efficient signal processing. The sampling rate of a signal must be at least twice as high as the signal's highest frequency to comply with the requirements of the theorem. It is necessary to take these steps to ensure that the signal can be perfectly recreated from its samples.

By using the Shannon-Nyquist theorem, we can design more efficient signal processing systems that only sample the necessary frequency components and ignore

the rest, reducing the quantity of data that has to be processed. This leads to lower computational and storage requirements, making the signal processing more efficient.

Sparse recovery approaches' objective is to recreate a signal from a small amount of undersampled data. Sparsity is a method that has been widely used because of its efficiency in a variety of signal-processing applications. Some examples of these applications include statistical analysis, classification, and data compression. When a signal is represented using a sparse basis, like the discrete cosine transform, wavelet, or curvelet, among others. It is classified as a signal that can be compressed. In the sparse representation domain, the signal samples can be interpreted as data observations. A linear modification of the movement ultimately leads to the production of the light signal representation.

The ability to reconstruct sparse signals with significantly fewer observations than the standard sample size has recently been demonstrated. This is main development in signal processing field. It would be necessary to cover all of the signal's available bandwidth. The result of methods for locating the sparsest approximation from duplicated dictionaries has made it feasible to achieve this goal. The efficacy and efficiency of sparse signal recovery have been significantly improved due to these strategies. The class of algorithms known as "greedy iterative techniques" is the one that is the simplest while maintaining high-efficiency levels. The matching pursuit (MP) algorithm, the orthogonal matching pursuit (OMP) algorithm, and the compressive sampling matching pursuit (CoSaMP) algorithm are the three techniques that are used most frequently. [11], [12], [13] [14], [15], [16].

1.7 Sparse reconstruction applications

Sparse reconstruction have many applications such as

- Information processing.
- Data compression

- Optical imaging
- Radar signal processing
- Channel estimation in wireless Communications
- Medical Imaging

1.8 MUSIC Algorithm

The acronym MUSIC stands for "Multiple Signal Classification," In signal processing; it is a well-known technique for calculating the direction of arrival (DOA). MUSIC method uses a subspace-based technique to identify the noise subspace and then estimate the DOAs by looking for the peak in the spatial spectrum of the signal. This is the fundamental concept behind the algorithm. To speak more specifically, the MUSIC method extracts the signal subspace and the noise subspace by using the eigenvalue decomposed of the correlation matrix containing the received signal. The next step is to create what is known as a steering vector, which is a representation of the reaction of the array to a signal that has arrived from a particular direction. The program can estimate the DOAs by projecting the noise subspace onto the orthogonal complements of the signal subspace and then finding the directions corresponding to this projection's lowest eigenvector. This allows the algorithm to determine the DOAs. Music can be utilized in various applications such as sonar, radar and wireless communication networks to determine the direction of incoming signals.

1.9 Problem Statement

The objective is to determine the angle and range of target through the use of sparse reconstruction techniques in a FDA MIMO radar system.

1.10 Summary Of Contributions

The central focus of this thesis is on Sparse reconstruction algorithms applied on FDA MIMO radars and to compare the performance of various sparse reconstruction algorithms for the target parameters estimation (range and angle) in FDA MIMO radar. Algorithms including NESTA, FBMP and OMP were applied on FDA MIMO radar. The results of the recovery were analyzed in the form of MSE verses SNR for target parameter estimation. The significance of selecting an efficient sparse recovery technique to improve sparse signal estimation performance and to find better way to accomplish the radar signal acquisition and processing with a considerably small amount of data and power requirement.

1.11 Thesis Arrangement

The thesis is divided into 5 chapters the contents of these chapters are summarized below:

1. Chapter 1 is the introduction of Radar and its types, sparse reconstruction and Music algorithm. It consists of problem statement and the summarizing contents of thesis.
2. Chapter 2 consists of the literature review.
3. Chapter 3 is based on the Sparse Reconstruction Algorithms.
4. Chapter 4 is based on the proposed Methodology.
5. Chapter 5 consists of conclusion.

CHAPTER 2

Comprehensive Review of the Literature

2.1 Frequency Diverse Array Radar

The author provides an overview of FDA and its potential for use in radar and navigation applications. The basic structures of FDA systems are presented in [17], as well as a comparison to traditional phased array methods. Recommendations for selecting suitable system characteristics and implementation are also discussed. The author also describe the potential applications of FDA radar, including cognitive FDA radar, identification FDA radar low probability, assessment of the distance and angle of targets, and identification of technological problems.

The author in [18], provides information on a Frequency Diverse Array that uses a frequency offset that increases logarithmically and produces a beam pattern with a single maximum at the target point. It also includes mathematical descriptions and evaluations of the transmitter for this radar system. The authors also present the transmit beam pattern, which they compare to those of a phased-array radar and current FDA designs with uniform frequency offset. The author worked on uniformly spaced linear FDA only and the angle was obtained, as they only worked on angle and didnot involved FDA MIMO radar.

The author in [19] suggests using time dependent frequency offset to generate a

beam pattern that is stable over time for a specific range and even angle combination. Simulations show that, although the beam pattern still varies for other range and angle pairs, it remains constant for a particular distance and angle pair. The target detection can be improved by constantly illuminating the target throughout the pulse duration in the suggested radar system, resulting in a strong reflection. It provides simulation results to demonstrate the effectiveness of the proposed approach. However, it lacks experimental validation of the proposed method, which could have further strengthened the findings.

By providing an array factor that depends on range, direction, and time, this increment makes it possible to target energy delivery to a specific range and angle. Antennas that use frequency diversity are compared to phased arrays by the author of [20], who offers an overview of the two types of arrays. At each element, the FDA makes use of frequency adjustments that are pretty minor compared to the array's carrier frequency. In addition, the author analyzes the possible applications of the FDA in spectrum energy control and the technical obstacles connected with implementing it into effect. This is to encourage more research on technology relevant to the FDA. The author does not compare frequency diverse array antennas with other existing antenna technologies, which could provide readers with a better understanding of the advantages and limitations of this technology compared to other alternatives.

The author in [21], conducts research on three fundamental receive chain architectures, analyzes their spatial patterns, and assesses the complexity of their designs while operating in a specific setting with a single target. The author also provides a concise description of a receive pattern in closed form. The author does not compare the proposed receiver architectures with other existing receiver technologies, which could provide readers with a better understanding of the advantages and limitations of the proposed architectures compared to other alternatives.

In [22], a thorough analysis of the FDA signal characteristics was carried out. The author also examines the transmitted and received signals, with a focus on topics such as Doppler effects, the ambiguity function, and inter element spacing

of array. Furthermore, it briefly discusses different waveforms and introduces the concept of a waveform diverse array. [22]. The author did not worked with FDA radar combined MIMO.

The author in [23] suggests that Ground-Moving Target Indicators (GMTI) processing might benefit from using linear Frequency Diverse Arrays (FDA). It is well known to have trouble reducing ambiguous range clutter. In a linear FDA, each channel works at a distinct frequency, and this results in the formation pattern that relies on the range. The output SINR in the area of ambiguous clutter Doppler is considerably boosted when FDA is used, which indicates improved detection. It has been demonstrated that the SINR of the output may potentially increase by up to 40 decibels, as contrasted with an array with a constant frequency. It did not detect the target with high probability moreover the error was more in this cited technique.

The author in [24] explores the application of planar array geometries to beamforming theory in FDA and presents snapshots of spatial pattern from both the transmit and receive sides. While FDA has been discussed previously as a linear array on transmit or with a receiving processing chain that omits some transmitted signals, the author suggests a method that allows each element to observe and interpret every transmitted signal in a monostatic arrangement. This method enables a more complete analysis of the FDA system and its potential applications. This system did not allow the receiver to maximize the signal-to-noise ratio for the available power and main beam peak-to-side ratio was not improved. It does not provide experimental results to demonstrate the effectiveness of the proposed receiver architecture in real-world scenarios. This could limit the confidence of readers in the potential of the proposed architecture.

The author in [25] proposes a joint two dimensional Inverse Synthetic Aperture Radar (ISAR) deception technique based on FDA and interrupted sampling. FDA permits more creative flexibility than the conventional methods of producing range deception, such single channel and phased array approaches. The suggested strategy produces a collection of erroneous targets in both range and cross-range direc-

tions. Advantage of this technique is that regulating the amount and distribution of these fake targets is easy, very effective, and needs very little processing work. It is anticipated that using this combined method will improve ISAR systems' performance by making it more difficult for prospective adversaries to recognize and categorize targets. Computational burden was not improved as this technique did not worked on finding the range.

A Multi-Layer Perceptron (MLP) neural network is used in a method reported in [26] for estimating the combined range and angle for FDA. The MLP model is built using signal data generated by an optimal outcome of the FDA radar system. The effectiveness of the training MLP neural revenue is demonstrated through experimental assessment. Because of this technology, it is projected that FDA radar systems will have improvements in terms of their efficiency as well as their accuracy when estimating angles and distances. Additionally, there is a possibility that the computational complexity of the signal analysis required for target recognition and detection will be reduced due to this method. This technique didnot use FDA with MIMO moreover the algorithms of sparse reconstruction were not applied.

The author in [27] proposed an FDA synthesis technique for designing the transmit beampattern based on range and angle using offset of frequency optimization. To realize a transmit beampattern in the form of a dot, the suggested approach uses optimization using particle swarms in designing the FDA element frequency increment. In addition, temporal modulation compensation was considered while designing matched weights. Compared to prior FDA frameworks, the suggested technique displayed increased time-invariant efficiency. The range– angle dependence is not decoupled and computational complexity is not reduced.

In [28], the author proposes a method to address the time varying issue in the receive beamforming of FDA. This method provides increased flexibility by removing the constraint on pulse duration, resulting in improved receive beamforming efficiency. It does not provide experimental results or simulations to validate the corrections proposed. This could limit the confidence of readers in the effectiveness

of the corrections.

The author in [29] introduced a novel FDA radar system that employs diverse linear frequency modulation waveforms. The receiver architecture incorporates a time variant beamforming chain and maintains the FDA system's automatic spatial beam scanning capability, enabled by the increment in frequency across elements. However, the current receiver based beamforming used in FDA systems can lead to low echo energy signal tolerance or high sidelobe peaks during target recognition. This paper primarily presents theoretical analysis and simulations. However, it lacks experimental results to validate the proposed waveform design method. This may limit the confidence of the readers in the effectiveness of the proposed approach.

A symmetric FDA with a Hamming window that is uniformly spaced is presented by author in [30], which employs tapering inter element offsets of frequency. With this configuration, a single maximum beam pattern pointed in the desired range and angle values is produced. One potential con of this paper is that it may have a limited scope. The authors focus only on beam pattern synthesis for an FDA radar with Hamming window-based nonuniform frequency offset. While this approach may be effective for this particular scenario, it may not be suitable for other radar systems or applications.

The applications of frequency diverse arrays in bistatic radar are examined in [31] and [32], with the latter using linear frequency modulated continuous waveforms for the FDAs. In [33], a full wave simulation of an FDA antenna is presented, utilizing the finite difference time domain technique to investigate the radiation pattern characteristics of changes in offset of frequency, element spacing, and array size. A mathematical analysis of the LFM CW FDA is developed to provide a fundamental proof-of-concept structure. Additionally, the multipath effects of the FDA over a ground plane are explored in reference [34].

The authors in [35] examined the phase characteristics of a FDA based on a suggested generalized structure. They derived a closed form signal model and phase radiation pattern, as well as a phase radiation function, based on the structure.

Authors then investigated periodicity radiation pattern of phase using a recursive method and rational analysis. Finally, phase center of generalized FDA was calculated using a three point technique. Considerable numerical results were obtained to validate the proposed signal model. The proposed approach does not introduce any significant novel concepts or ideas to the existing literature on phase characteristics of frequency diverse array radar. The paper primarily describes an approach that builds upon existing techniques and methods.

For random log FDA radar, which shows range and angle dependency, a method has been given for creating the beam space transformation matrix based on the received signal. Its behavior is dependent on the range as well as the angle. It has been proved that the intended beam spatial transformation matrix does, to a significant degree, satisfy the beam gain criteria. However, the planned transformation matrix has a few flaws that must be addressed. For example, unclear beam gain and same peak power sidelobe levels. An optimization strategy was suggested by the author in [36] to overcome these concerns, which involves adjusting the array's element spacing and the random frequencies offset values to reach the optimal beam gain. The proposed algorithm is relatively complex and may require a high computational cost, especially in real-time applications. Therefore, it may not be practical for implementation in certain scenarios.

A nested FDA design scheme that combines angle and range dependent beam patterns and increased degrees of freedom in a nested array configuration. Due to source correlation, the commonly used multiple signal classification technique is ineffective in estimating multiple sources in this case. To address this limitation, an algorithm based on CS range and angle estimation was suggested in [37]. This suggested approach utilizes fewer snapshots and outperforms conventional spatial smoothing (SS) based localization methods.

The author in [38] proposed a clutter suppression technique for blind Doppler target recognition in FDA radar by utilizing the Doppler spreading effect. A joint angle and range Doppler processing system is developed for FDA radar that takes the Doppler spreading effect into account. The Doppler spreading effect offers

the potential to resolve Doppler ambiguity. For target detection utilising FDA, the probability of detection and the signal to clutter plus noise ratio are also calculated.

In [39], author presents a restudy of the literature on designing a time-invariant beam pattern for FDA radar to concentrate transmit energy in a specific location. The author reexamined the derivation of the FDA beam pattern synthesis and discovered a neglected constraint condition. After comparing the results of prior work with the author's results, it was concluded that it is not possible to obtain a beam pattern that solely focuses on specific spatial positions and persists for a particular duration.

The range and angle matched receiver is a novel form of receiver introduced by the author in 40. The transmit beam pattern modulates a range and angle dependent filter that the receiver uses to process each shorter sub pulse after breaking the pulse duration into multiple shorter sub pulses. The author looked into the characteristics of the ambiguity function in various dimensions and provided a design for the sub pulse duration.

In [41], a signal transmission system for bistatic frequency diverse array radar is proposed, which aims to detect and localize targets accurately while keeping the computational complexity low. The proposed approach aims to provide the narrowest possible transmit beam for a given number of transmit antennas, and achieves better detection and localization performance compared to existing methods. The approach uses a fast algorithm to generate initial estimates that can be used to initialize a numerical algorithm for computing the maximum likelihood estimates.

A method for designing a general receiver for FDA radar was suggested in [42]. The suggested receiver signal model can accommodate any FDA radar with arbitrary frequency and geometry increments. By utilizing the maximum likelihood criterion, the best estimate and detection may be made with the suggested receiver structure.

In [43], a model was developed to analyze the structure of interference covariance

matrix for spectral interference in FDA radar. The study showed that FDA radar has the potential to reduce spectrum interference, even if it enters via the receiver's main lobe, as the study indicated. The author described an approach that improves the output SINR to build a transmit weight vector that employs adaptive element-wise power allocation. Specifically, this approach aimed to improve the SINR. According to the research findings, the FDA radar that was outfitted with different power allocations can avoid spectral interferences by adjusting the spectrum across which it broadcasts. Traditional phased array (PA), multiple input multiple outputs (MIMO), and uniform power allocation radars all displayed signal-to-noise ratios that were inferior to those achieved by the FDA radar with adaptive power allocation.

2.2 Frequency Diverse Array MIMO Radars

The author in [44] examines a system of MIMO radar that uses beamforming of transmits antenna and receive antenna with a radar signal to produce sparse radar scene with frequency domain. The next step is to create the radar waveforms and receiver filters to recreate the radar picture using compressed sensing techniques. These approaches identify several extended objects whose impulse responses are known. The MIMO radar system's performance for target identification depends on the reconstruction of a noisy scene to get optimal results. This accuracy is determined by analyzing the results of numerical examples acquired from simulations.

The authors of [45] proposed a model for performing frequency diverse array with MIMO radar operation and embedded communication using Costas frequency codes. They employed phase shift keying to embed communication symbols in each of the Costas frequency codes and used standard ratio testing at the receiver side to recognize the embedded symbols. Model was evaluated based on the symbol error rate; transmit beam pattern, SINR, and data rate for communication. The findings show that the suggested model can effectively produce low probability of

interception in radar applications.

The authors of [46] investigated the target detection performance in frequency diverse array radar MIMO, which combines benefits of the FDA even MIMO radar for single coherent pulses and even for multiple coherent pulses. They developed target detection signal models for FDA MIMO, phased array, FDA, and MIMO radars and used a unified framework detector based on the Neyman Pearson criterion to compare their target detection performance based on target detection. Moreover, to compare their performance, the SINR and the deflection coefficient are also used as performance metrics. Better target detection performance is achieved by FDA MIMO radars as compared to other conventional radar systems.

In [47], the authors proposed a joint disambiguation technique based on the estimation of signal parameters via rotational invariance techniques (ESPRIT) for LBTA-FDA-MIMO radar. They proved a uniqueness theorem to address the challenge of the existence of ambiguities in both range and angle. The proposed technique was evaluated using simulations and demonstrated improved estimation accuracy of both angle and, more importantly, ranging accuracy.

The author of [48] suggested a search-free approach for estimating range and angle in monostatic MIMO radar with FDA by using an estimate of signal parameters through the rotational invariance methods (ESPRIT) algorithm. This algorithm was used to calculate the components of the signal. The angle was estimated with the algorithm's help, and the concept of least squares determined the spectrum.

The author of [49] developed a 1D MUSIC strategy for merging range estimates and angle estimations in monostatic MIMO radar incorporating FDA. Suggested approach was developed to reduce the amount of computational complexity while obtaining performance levels equivalent to those of the 2D MUSIC algorithm.

Range and angle calculation in general FDA MIMO radar using MUSIC algorithms, the authors found Cramer-Rao lower limits and mean square error formulas. These formulas can be found in [50]. In addition, they figured out the range and angle resolution requirements essential for target recognition and localization. The research indicates that FDA-MIMO radar performs better than traditional

MIMO radar regarding the range-angle seismic performance evaluation and the resolving thresholds performance.

In [51], author suggested a combined range and DOA estimation method in monostatic MIMO radar with FDA. Suggested technique derives its functionality from the forecast of signal parameters using rotationally invariant techniques. Using accurate data helps improve the accuracy of estimations and reduces the amount of computing complexity. The rotation invariance of the receiving subarrays is taken advantage of so that the connection between range and angle in the transmitting array steering vectors may be avoided. This allows the DOA to be estimated. Also, the author suggested a method to eliminate the phase ambiguity brought on by the transmitting array steering vector.

MIMO radar has several advantages, including enhanced gain in both DOFs and spatial diversity. Unfortunately, it has difficulty correctly differentiating targets that are densely grouped inside the same angle cell but separate range cells. The FDA MIMO radar was proposed to address this problem by taking advantage of its range dependent beampattern for target estimation for range and angle. However, as this is a recently developed radar technique, it requires theoretical performance analysis. The CRLB and MSE equations for range and angle estimation methods based on the MUSIC approach, commonly employed in the bulk of FDA MIMO literature, are derived by the author of [52]. These expressions may be found in the cited article. In addition, the author devises target detection and localization criteria to maximize range resolution and angle accuracy.

In [53], the author investigates the challenge of adaptive target detection using MIMO combined with FDA radar in the presence of homogeneous Gaussian interference. This work investigates the development of adaptive detectors based on the generalized likelihood ratio test (GLRT) criteria. The test assumes that the target's location concerning each range cell is uncertain. The Newton method, discrete grid search, and semi-definite programming are the three optimization procedures used in this work to estimate the maximum likelihood of the incremental range of the goal while operating under the H1 hypothesis (SDP). At the

analysis step, both the recently developed adaptive detectors and the mismatched receivers are tested, assessed, and compared concerning their performance in terms of detection.

Using a FDA as the transmit array and a MIMO radar; author attempt to detect the target signal's presence while rejecting any potential deceptive jamming. The GLRT was utilized to address this issue. In [54], the author characterized the potential false target locations during the design phase. FDA MIMO radar provides controllable DOFs in both the angle and range domains, range and angle relationships can be used to reject false targets resulting from mismatches either in angle or range. In the analysis stage, the detector's performance was compared to that of a conventional MIMO scenario to evaluate its effectiveness in the presence of ECM systems, especially when dealing with mainlobe deceptive jamming.

In [55], the author suggested a technique for estimating joint angle, range, and Doppler for FDA MIMO radar. Rather than starting with the maximum likelihood (ML) estimator, the approach uses the extended invariance principle to estimate the Doppler independently, which reduces computational complexity. Then, an unstructured model is applied to separately estimate the range as well as angle. As a direct consequence, the challenge of joint estimation is broken down into three different search problems in a single dimension. The numerical outcomes show that the suggested approach has significant advantages over traditional machine learning algorithms.

A persymmetric adaptive detector for FDA MIMO radar is proposed in [56], assuming an unidentified Gaussian interference-noise covariance matrix. The proposed method in [56] involves obtaining an unbiased estimate of the interference noise covariance matrix by leveraging its inherent structure. Using this estimate, an analytical expression for the detection probability is derived. The study's numerical findings show that the persymmetric adaptive detector beats its traditional equivalent for FDA-MIMO radar.

PSFDA-MIMO radar, which combines polarization sensitive frequency and FDA MIMO, is a relatively new technology. However, current algorithms for parameter

estimation with this radar require computationally expensive multidimensional searches. In [57], the author introduces a search free method for estimating 4D parameters with PSFDA MIMO radar. DOA is calculated using the rotational invariance of the receiving array and the Estimation of Signal Parameters via Rotational Invariance Techniques (ESPRIT) algorithm. Then, using the rotational invariance of the transmitting array and the estimated DOA parameter, range is estimated via ESPRIT. Finally, the ESPRIT algorithm is used again with the rotational invariance of the polarization domain to calculate polarization parameters. This method is called the successive ESPRIT algorithm, and the results of the simulation demonstrate its efficacy for PSFDA-MIMO radar.

In [58], the author proposes a robust adaptive beamforming technique for FDA radar combined with MIMO using FDA as transmit array. The suggested approach utilizes the direct data domain technique, which includes a smoothing process in both the transmit and receive domains to reduce the effect of the target. This results in three homogeneous samples that can be processed further using secondary data from multiple pulses. The FDA MIMO radar system leverages the combined transmit and receive domains to separate the interference from the target signal. The simulation results presented in the study demonstrate the effectiveness of this approach.

The author presents a combined range angle estimate strategy for FDA MIMO radar based on gridless compressed sensing [59]. This method was conceived and created by the author. This explains a decoupling model to decouple the range from the angle. Following that, the problem of scope and angle calculation is rethought as a problem of atomic norm minimization (ANM) in two dimensions. After that, singular value decomposition (SDP) problem is constructed from it with the help of convex relaxation. To address the SDP problem, the author developed an estimation method that leverages the accelerated proximal gradient (APG) technique. The superior performance of the approach that was provided was shown with the use of numerical simulations.

With a low cognitive probability of intercept (LPI), the author in [60] proposes a

broadcast beamforming technique. This scheme is built on a hybrid array antenna that comprises FDA and MIMO technologies. According to [60], this scheme was suggested by the author. Consequently, the FDA MIMO radar's one of a kind transmitting beampattern, which is dependent on both range and angle, it is possible to minimize beam power at the target location in order to make it less visible while at the same time increasing beam power at the radar receiver in order to maintain radar detection performance. This strategy allows for the achievement of LPI. In addition, FDA radar with MIMO has a cognitive mode of operation, which estimates the target range and direction of approach by using numerous signal classification algorithms in a two-dimensional space. After that, these estimations are sent to the transmitter so that the FDA MIMO transmits beamforming may be updated. Optimization of transmit beam-forming is a non-convex issue, and the authors provide three ways to tackle it: closed form solution, nonlinear combination, and linear combination. The results of simulations are used to validate each of the recommended strategies.

The author of [61] explains how the ESPRIT technique may be used for FDA MIMO radar. This technique can calculate the range and even angle between the objects. The recommended pairing strategy is used in order to sidestep the high degree of processing complexity connected with both the 2-D peak searching that is carried out by the MUSIC algorithm. Specifically, this complexity is avoided by using the word "sidestep." In addition, the author offers closed-form formulae for the average square error and the Cramer-Rao lower limit for estimations of angle or range. Both of these are presented in the previous section. The author has shown, through both theoretical analysis and empirical observations that FDA-MIMO radar performs at a level that is superior to that of traditional phased-array radar as well as MIMO radar when it comes to target localization.

In [62], the authors present an unambiguous technique for jointly estimating range and angle in MIMO radar systems with FDA. In contrast to conventional phased array radars, MIMO radars with FDA have the ability to use a small increment in frequency across the array elements, allowing the transmit steering vector to depend on both range as well as angle. Ability of FDA MIMO radars to use

frequency increments across array elements allows for exploitation of degrees of freedom in both the range and angle domains, enabling joint estimation of target range and angle parameters even in the presence of range ambiguity. In [62], authors derive the range and angle Cramer-Rao bounds and examine the coupling between these two parameters. The authors also provide numerical data that showcase the effectiveness of their suggested approach. These results indicate a superior estimation performance compared to conventional phased array and MIMO radars, particularly in scenarios that involve range ambiguity.

The method that is described in [63] is successful in overcoming the restrictions that FDA has for tracking moving targets and offers a solution for the combined processing of range, angle, and Doppler data for tracking low-observable moving targets under challenging settings. The SRD focus processing strategy is a hybrid method that combines the FDA and MIMO processing methods to use the strengths of both approaches. The SRD data are processed quickly and effectively using the STFD approach that has been presented, which also offers a high-resolution joint estimate of the range, angle, and Doppler parameters. Numerical simulations shows the suggested method is capable of effectively detecting and estimating moving targets, even in challenging scenarios. As a result, this method holds promise as a potential candidate for integration into future radar systems.

The author in [64] proposes using MIMO with FDA radar as the transmit array to suppress false targets for main beam deceptive jamming. The steering vector depends on both distance and angle in FDA-MIMO, allowing for mismatches in either range or angle to be used for false target suppression. The proposed scheme was shown to be effective in suppressing jamming in various situations through simulations.

2.3 Sparse Reconstruction

The BIM-NESTA technique is a regularization method that combines the Born Iterative Method with the NESTA algorithm to solve sparse microwave imaging problems. By using a first-norm penalty term and measurement data misfit in the cost function, the method can reconstruct closely spaced objects and preserve edges in a sparse domain. This has been supported by numerical simulations presented by the author in [65].

In [66], the author proposed a Bayesian matching pursuit (BMP) algorithm as a method for detecting sparse signals in a greedy manner. The BMP algorithm's primary objective is to determine which nonzero components of a sparse signal have the most excellent posterior probability over a series of iterations. The results of the simulation reveal that the BMP method is superior to the currently used strategies for sparse signal reconstruction in terms of frame error rates, despite the fact that it has a much lower level of computational complexity than other techniques.

The article's author [67] described a straightforward recursive method for calculating the most petite average square error using linear regression models. In this scenario, the prior vector of uncertain variables is represented by a Gaussian mixture. Using the just detailed approach, it is possible to acquire both an estimated MMSE estimation of the parameter and a set of mixing parameters with a high posterior probability. In order to demonstrate that the proposed strategy is effective and to draw attention to the differences, a numerical simulation was run between the MAP model selection procedures and the MMSE estimation.

OMP technique is a possible solution for recovering a high-dimensional sparse signal from a sparse group of noisy linear measurements. This may be accomplished by using the approach. In [68], the author provides an entirely data driven OMP approach with distinct stopping circumstances. The OMP approach can reliably recover the support for the movement despite the need for reciprocal incoherence as well as the lowest amplitude of the nonzero elements of the signal. This results

in a high likelihood of successful recovery. This can be accomplished with a high level of precision. In addition, the author examines the challenge of determining whether nonzero components are relevant in a scenario in which some of the nonzero features are likely to be of a low magnitude. The OMP approach would, despite the circumstances, nevertheless choose all of the relevant components before selecting the incorrect ones. By using updated stopping criteria, the OMP technique is able to provide an assurance that no zero members will be chosen.

In [69], the author proposed an OMP method for channel estimation, which aims to address the convergence issue encountered by the MP algorithm due to the reselection of basis vectors. By avoiding the reselection problem, the OMP algorithm has been demonstrated to produce more accurate channel estimates. When compared to the MP algorithm in the context of decision feedback equalizers based on channel estimates, the OMP algorithm has been found to outperform the MP algorithm while maintaining a similar level of computational complexity.

In [70], the author proposes a fast matching pursuit technique for sparse signal recovery that employs a Bayesian method. Unlike traditional methods, this approach can estimate sparse signals using Bayesian approaches even in situations where the prior signal is uncertain or otherwise not Gaussian. This method does not depend on the signal's statistics; instead, it uses the a priori demographics of frequency components and the signal sparsity rate. If the signal statistics are not readily accessible, these statistics might be deduced from the data. In order to find the sparse supports which are most dominant and to compute the estimated MMSE values of the sparse signal, this strategy makes use of a greedy methodology and order-recursive updates of its metrics. The outcomes of the simulation provide evidence that the estimation that was provided is both practical and reliable.

An effective strategy for resolving reconstruction issues involving sparse signals was given by the author of [71]. The proposed method is an augmented Lagrangian technique based on the dual problem. Due to the dual formulation, it is effective even when there are many more unknown variables than observations. Additionally, the sparsity in the solution is taken advantage of, and the primal

variable is explicitly updated.

In [72], there is a technique for sparse restructuring source estimation that makes use of a coprime array. A difference coarray is particularly produced from the coprime array, and a virtually uniform linear subarray co-variance matrix sparse restructuring optimization problem is designed for DOA estimation. This is done so that the number of degrees of freedom (DOFs) may be increased. Processing the recovered sparse spatial spectrum involves utilizing a refined sliding window approach to get rid of spurious peaks and employing a least squares problem to get a more accurate power calculation. The results of the simulation show that the suggested approach is successful in terms of estimating DOA and power, as well as the DOFs that may be attained.

Adaptive Sparsity Matching Pursuit (ASMP) is a novel greedy approach developed in [73] for sparse solutions to underdetermined systems that use a random projection matrix. Back tracking is used by ASMP to enhance both the currently used approximation as well as the supports that have been chosen. ASMP was developed to extract information on the sparsity of the target signal in an adaptive manner utilizing a stagewise technique. These improvements provide results that are even more attractive than those produced by the most advanced version of the CoSaMP algorithm, which works without any prior awareness of the sparsity level in the data. The experimental findings indicate that the proposed technique is efficient in handling input data, whether they are free from noise or contain noise.

A novel sparse recovery approach using weighted subspace fitting is suggested in [74] as a potential solution to the problem of DOA estimation. The approach that has been developed uses a regularization scheme that strikes a balance between the sparsity penalty and the subspace fitting error for all SNR ranges. Also, this algorithm is a modified form of the $l_1 - SVD$ algorithm. The efficiency of the suggested technique is shown by numerical simulations, especially in situations with a low signal to noise ratio.

The author shows an easy Bayesian technique for reconstructing sparse signals in [75]. This method uses the sparsity constraint and a priori statistical data,

regardless of whether or not these data are Gaussian, to obtain estimates that are close to being optimum. In addition, the author presents a new method for fast sparse recovery that capitalizes on the large structure of the sensing matrix, which is a component often used in various signal processing applications. In comparison to commonly used convex relaxation methods and greedy matching pursuit strategies. The approach that has been suggested has low computational complexity, especially at high sparsity levels.

DOA estimation using a sparse array based on CS was introduced in [76]. The sources are supposed to be at the off-grid location according to the receiving antenna array. By using the OMP method for reconstruction from the sparse samples, the grid-off DOA of the sources can be calculated almost accurately.

The authors above worked on uniformly spaced linear FDA and focused on obtaining angle information. They did not involve FDA MIMO radar, which is an emerging technology that uses multiple antennas to transmit and receive signals, and could potentially improve radar performance. Conventional phased array radars can suffer from range ambiguity, which occurs when the radar cannot distinguish between multiple targets at different ranges that appear to have the same Doppler shift. However, the ability of FDA MIMO radars to use frequency increments across array elements allows for exploitation of degrees of freedom in both the range and angle domains, enabling joint estimation of target range and angle parameters even in the presence of range ambiguity. The main focus of this thesis is on Sparse reconstruction algorithms applied on FDA MIMO radars which is the novel idea and to compare the performance of various sparse reconstruction algorithms for the target parameters estimation that are range and angle in FDA MIMO radar. Algorithms including NESTA, FBMP and OMP were applied on FDA MIMO radar. The significance of selecting an efficient sparse recovery technique to improve sparse signal estimation performance and to find better way to accomplish the radar signal acquisition and processing with a considerably small amount of data and power requirement.

CHAPTER 3

Sparse Reconstruction Algorithms

3.1 Sparse Reconstruction

Sparse reconstruction is an approach for reconstructing k -sparse data. Most real signals can be considered sparse in some domain. Such signals have large number of elements which are equal to or close to zero.

3.2 Reconstruction of Sparse Signal

To retrieve the complete signal from a limited number of measurements, a set of N coefficients $X(k)$, where $k = 0, 1, \dots, N - 1$, is used. The vector containing these coefficients, referred to as \mathbf{X} , is classified as sparse if the count of its non-zero coefficients, represented by K , is significantly lower than the total number of samples, N .

$X(K) = 0$ for $K \notin \mathbb{K} = K_1, K_2, \dots, K_k$ and $K \ll N$.

The count of non-zero coefficients is represented by $\|\mathbf{X}\|_0 = K$ and is known as the l_0 -norm of the vector \mathbf{X} . A measurement of \mathbf{X} can be expressed as a linear combination of its elements $X(k)$, with the m th measurement represented

by $y(m)$. If there are M measurements, a set of M linear equations can be written as follows:

$$y(m) = \sum_{k=0}^{N-1} \alpha_k(m) \mathbf{X}(\mathbf{k}), m = 0, 1, \dots, M-1, M < N \quad (3.2.1)$$

The coefficients for the measurements are denoted by $\alpha_k(m)$. We can represent the set of linear equations in matrix form as follows:

$$\begin{bmatrix} y(0) \\ y(1) \\ \vdots \\ y(M-1) \end{bmatrix} = \begin{bmatrix} \alpha_0(0) & \alpha_1(0) & \dots & \alpha_{N-1}(0) \\ \alpha_0(1) & \alpha_1(1) & \dots & \alpha_{N-1}(1) \\ \vdots & \vdots & \ddots & \vdots \\ \alpha_0(M-1) & \alpha_1(M-1) & \dots & \alpha_{N-1}(M-1) \end{bmatrix} \begin{bmatrix} X(0) \\ X(1) \\ \vdots \\ X(N-1) \end{bmatrix} \quad (3.2.2)$$

We can represent the sampled signal as a vector.

$$Y = Ax + v \quad (3.2.3)$$

The measurement matrix is denoted by the matrix A , with its elements represented by $\alpha_k(m)$. The vector v represents any additional noise present in the system. Our objective is to retrieve the vector x from the equation $Ax = y$. To achieve this, various reconstruction algorithms are applied.

3.3 Nesterov's Algorithm (NESTA)

This algorithm provides a speedy and precise solution to common recovery problems in signal processing. The linear model is considered as follows:

$$b = Ax_o + z \quad (3.3.1)$$

where x_o is the interest signal. z is the noise. A is a known $M \times N$ sampling

matrix.

Input :

A which is measurement matrix with $M \times N$ dimensions. b is the Observed data with a $M \times 1$ array.

Output :

x_k is the estimate of the solution x_o on which *nesta* is applied.

3.3.1 Algorithm

The code solves the following optimization problem:

1.

$$\min_x \|Ux\|_1 \text{ s.t. } \|b - Ax\|_2 \leq \delta \quad (3.3.2)$$

Where U is a diagonal matrix and the measurement matrix is b . A is the matrix of normally distributed random numbers with dimension of $M \times N$ and K are the nonzero elements in x_0 and a signal $\mathbf{b} \in \mathbb{R}^N$.

2. The signal that we are attempting to recreate is x .
3. The SNR is set to a certain value, which is converted to a linear value. The code first generates the measurement vector b from a randomly generated sparse x_0 and a measurement matrix *Amatrix* with some added Gaussian noise.
4. The original signal is extracted from the noisy measurements using the NESTA algorithm, with the regularization parameter λ selected according to the noise level.
5. The algorithm is run several times for different SNR levels and iterations. Finally, the solution x_0 is plotted against the original signal, and the relative norm difference is calculated.

3.4 Results of Simulation

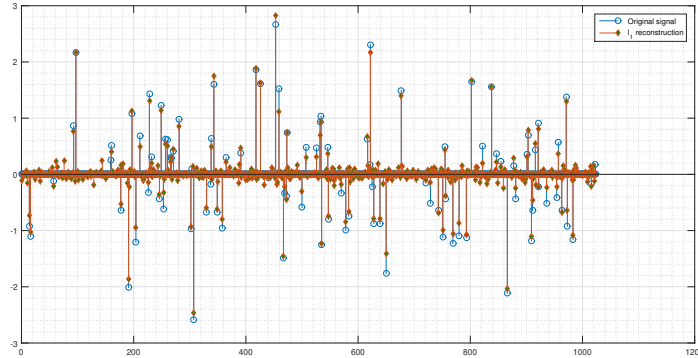


Figure 3.1: Reconstruction of Signal

The 3.1 figure above depicts reconstruction of a signal using NESTA Algorithm. The signal is reconstructed using l_1 normalization problem under a quadratic constraint using the Nesterov algorithm. The parameters used in this algorithm are U is the diagonal matrix, measurement matrix is b . A is the matrix of normally distributed random numbers with dimension of $N = 1024$ and $M = 512$ and with $K = 102$ those are the nonzero elements in x_0 and a signal $\mathbf{b} \in \mathbb{R}^N$. The SNR ratio is set to SNR dB = 50 dB, which is converted to a linear value. The original signal and the recovered signal are then compared and relative l2 norm difference between the two is printed. The script is written to perform this process multiple times with different SNRs, and reports the total number of function evaluations required by NESTA for each run.

The 3.2 figure depicts SNR Vs MSE graph using the NESTA Algorithm. The algorithms used $N = 1024$, $M = 512$ and $k = 102$. The performance of MSE is examined with 100 trials. When SNR is 0 dB in NESTA, MSE equals 1.45 dB. The MSE is 1.19 dB when the SNR is 2 dB. The MSE is 0.95 dB at 4 dB SNR. The MSE is 0.21 dB at an SNR of 18 dB. The average time for run of this algorithm was 2296.1 seconds and averaged error was 0.2126.

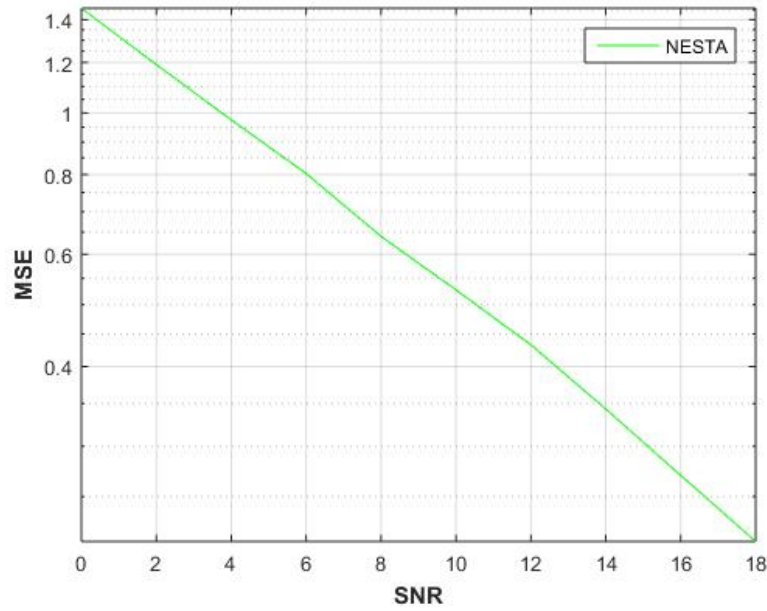


Figure 3.2: Nesta Algorithm SNR Vs MSE grap

3.5 Fast Bayesian Matching Pursuit

The difficulty of sparse signal reconstruction motivated developing a Fast Bayesian Matching Pursuit (FBMP) technique. This method estimates the sparse signal by choosing the best model and averaging the results. Sparse vector is represented as a combination of several different components; these components are chosen depending on the successive expansion of the model. Under the assumption of a binomial prior for the signal's sparsity, FBMP provides an approximation of the Bayesian MMSE estimate of the sparse vector, a multimodal Gaussian prior for the noise, and a multivariate Gaussian prior for the values of the sparse vector that are not zero. FBMP employs iterative greedy techniques to obtain a practical approximation of the MMSE estimator.

Consider observing the linear regression model as

$$b = Ax_o + z \quad (3.5.1)$$

We consider a linear model where the measurement vector \mathbf{b} with dimension M is related to an unknown parameter vector x_o , matrix A , and additive white Gaussian

noise with variance σ^2 . To account for sparsity, we model the parameters using a Gaussian mixture density.

Input :

b is the vector of observations of length M

A is the measurement matrix with $M \times N$ dimensions.

Output :

xmmse is the approximate sparse MMSE estimate of x_o , given b

3.5.1 Algorithm

1. The algorithm constructs a signal based on a given signal model and recovers the signal using the Fast Bayesian Matching Pursuit (FBMP) algorithm.
2. An observation vector is generated from a random mixing matrix and a sparse coefficient vector, which is generated using a user defined signal model.
3. The user can choose between a zero-mean binary model and a non-zero-mean ternary model for the signal.
4. The signal model is characterized by the means (μ_s) and variances (σ_s^2) of the coefficients.
5. To generate an observation, a sparse coefficient vector x is first generated with values drawn from the Gaussian distributions defined by the signal model. The observation is then generated by multiplying the coefficient vector with a random normal mixing matrix A .
6. The Signal-to-Noise Ratio (SNR) is specified in dB.
7. The FBMP technique is used to retrieve the sparse coefficient vector from the observation.
8. The function (FBMPR) is called to perform the recovery.

9. The code performs the experiment for different SNR values and for a specified number of iterations.

3.6 Results of Simulation

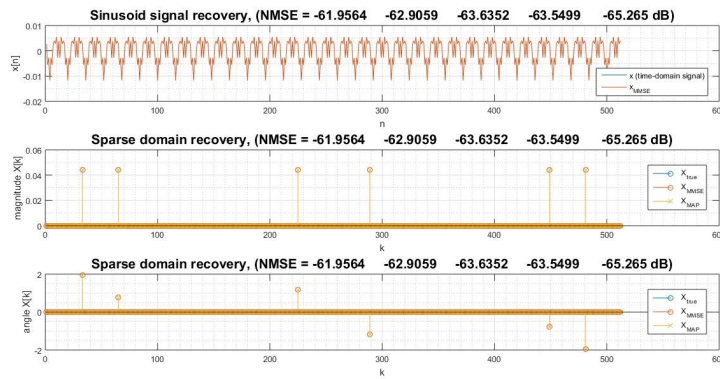


Figure 3.3: Reconstruction Signal of FBMP Algorithms

The figure 3.3 shows the reconstruction signal using the FBMP Algorithm. The results of the FBMP algorithm depend on the input signal and the parameters used for the algorithm. In general, the algorithm tries to recover a sparse representation of the input signal using a minimum number of measurements. The output of the algorithm is a sparse vector that represents the signal. The performance of the FBMP algorithm is evaluated based on the recovery accuracy and the speed of the algorithm. The recovery accuracy is a measure of how close the output vector is to the true sparse representation of the signal. The speed of the algorithm is measured in terms of the number of iterations required for convergence.

The 3.4 figure shows SNR Vs MSE graph using the FBMP Algorithm. The algorithms used $N = 1024$, $M = 512$ and $k = 102$. The performance of MSE is examined with 100 trials. In FBMP, When SNR is 0 dB the value of MSE is 1.169. When the SNR is 2 dB the MSE is 0.68 dB. when SNR is 4 dB the MSE is 0.53 dB. When SNR reaches to 18 dB is MSE is 0.065. Moreover, the average time for run of this algorithm was 2522.4 seconds and averaged error was 0.0605.

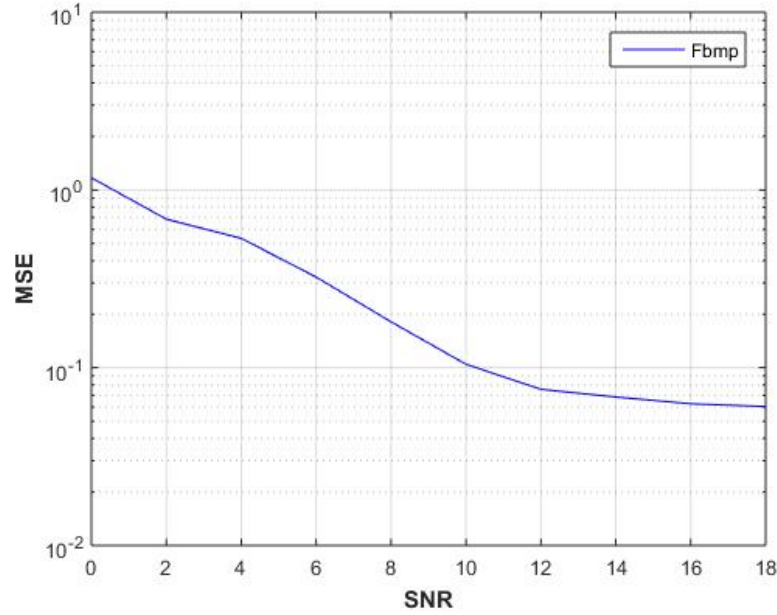


Figure 3.4: SNR Vs MSE graph of FBMP Algorithm

3.7 Orthogonal Matching Pursuit

OMP is a greedy technique built on Matching Pursuit (MP) algorithm that at each iteration removes the selected column vector from the residual vector. It constructs an approximation by going through an iteration process. Optimum solution is calculated at each iteration. This is accomplished by selecting a group of chosen columns from A , adding the column vector that most closely matches a residual vector r , that is, $r = b$. This cycle will continue. By projecting the vector b onto the space covered by the chosen columns in the set, the method will update the residuals. The residuals are orthogonal to all the chosen columns after each step. As a result, no column is picked more than once, and collection of selected columns grows with each step.

Input :

The matrix A represents the measurements, while the vector b contains the observations. Additionally, the variable k represents the approximation of the sparsity.

Output :

The estimated unknown signal's k -sparse value is x_0 .

3.7.1 Algorithm

1. A random Gaussian measurement matrix A is created with dimensions $M \times N$, where M and N are selected to be 512 and 1024, respectively.
2. A sparse signal x is generated with K non-zero elements, where K is chosen to be $M/5$, and it has a size of $N \times 1$.
3. Gaussian noise is added to the signal.
4. The Orthogonal Matching Pursuit (OMP) algorithm is applied to recover the signal.
5. An oracle solution is computed to compare the recovery error.
6. Results are displayed for each iteration, including the error in the recovered signal and the time taken for each algorithm to run.

3.8 Results of Simulation

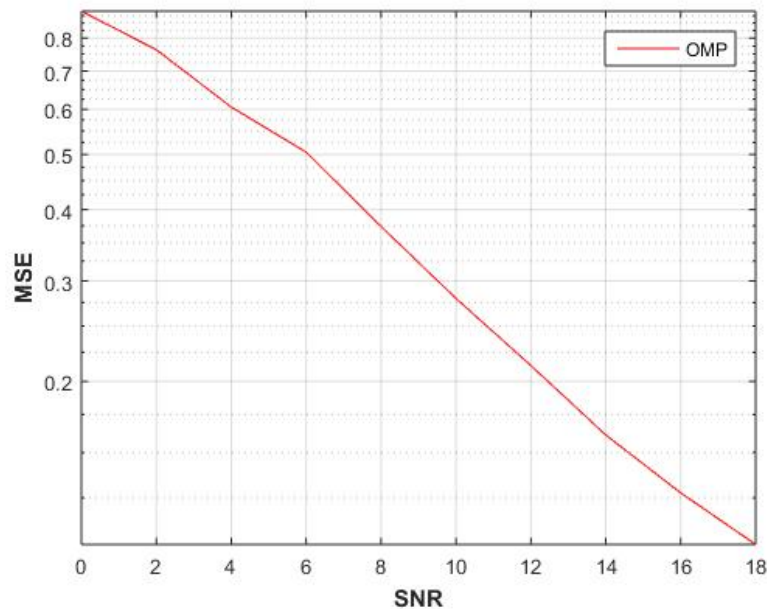


Figure 3.5: SNR Vs MSE graph of OMP Algorithm

The 3.5 figure depicts SNR Vs MSE graph using the OMP Algorithm. The algorithms used $N = 1024$, $M = 512$ and $k = 102$. The performance of MSE is examined with 100 trials. In OMP When SNR is 0 dB the value of MSE is 0.89 dB. When the SNR is 2 dB the MSE is 0.769 dB. when SNR is 4 dB the MSE is 0.605dB. When the SNR is 18 dB the MSE is 0.121dB. Moreover, the average time for run of this algorithm was 1336.3 seconds and averaged error was 0.0970.

3.9 Simulation Results of Different Algorithms

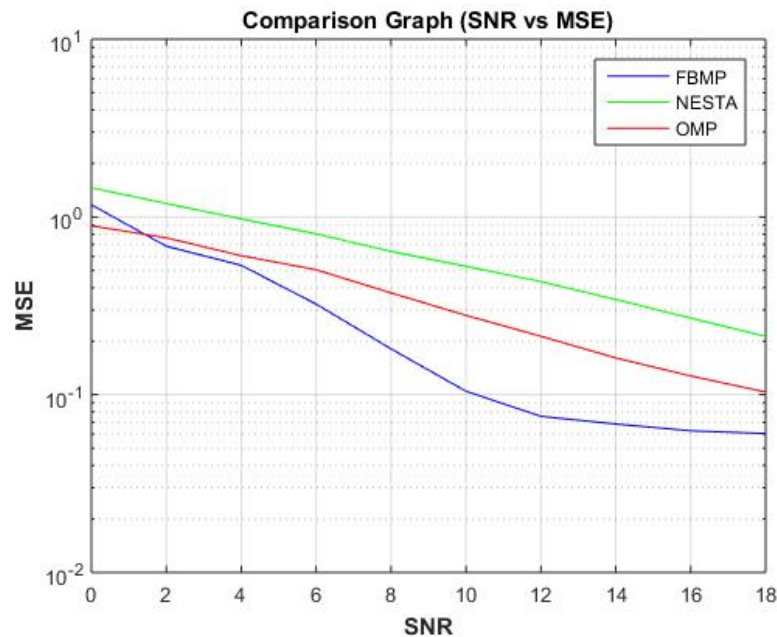


Figure 3.6: Comparison between different algorithms.

The MSE performance versus SNR of three distinct methods is depicted in Figure 3.2. The algorithms used $N = 1024$, $M = 512$ and $k = 102$. The performance of MSE is examined with 100 trials. The difference in performance of these algorithms is more noticeable. When SNR is 0 dB in NESTA, MSE equals 1.45 dB. The MSE is 1.19 dB when the SNR is 2 dB. The MSE is 0.95 dB at 4 dB SNR. The MSE is 0.21 dB at an SNR of 18 dB. In FBMP, When SNR is 0 dB the value of MSE is 1.169. When the SNR is 2 dB the MSE is 0.68 dB. when SNR is 4 dB the MSE is 0.53 dB. When SNR reaches to 18 dB is MSE is 0.065 and lastly, in

Table 3.1: Complexity analysis of Algorithms.

Algorithms	Average Error	Average time
NESTA	0.2126	2296.1
FBMP	0.0605	2522.4
OMP	0.0970	1336.3

OMP When SNR is 0 dB the value of MSE is 0.89 dB. When the SNR is 2 dB the MSE is 0.769 dB. when SNR is 4 dB the MSE is 0.605dB. When the SNR is 18 dB the MSE is 0.121dB. FBMP is is clearly the best performing algorithm. While OMP, however, performs a little bit better than the competition. The table above shows complexity analysis of different algorithms including NESTA, FBMP and OMP. It also shows the average error and average time.

3.10 Conclusion

In this chapter, we examine various popular sparse estimation algorithms, such as NESTA, FBMP, and OMP, for the purpose of recovering multiple sparse vectors from a set of noisy linear measurements that are underdetermined. The focus is on computing the MMSE and SNR estimates of the sparse vector, which provide a measure of estimation performance. Through numerical simulations, it has been shown that FBMP provides a good approximation to the MMSE estimator. OMP, however, performs somewhat better than NESTA. A number of sparse reconstruction issues can be solved using the adaptable and effective FBMP approach.

CHAPTER 4

Design and Methodology

We examined a monostatic FDA-MIMO radar that utilizes a uniform linear array consisting of half-wavelength spaced transmit and receive antennas. The system included M transmit antennas and N receive antennas, which were co-located to maintain consistent direction of departure (DOD) and direction of arrival (DOA). The transmit signal frequency of the m^{th} antenna was also analyzed.

$$f_m = f_c + (M - 1)\Delta f_o \quad (4.0.1)$$

we assume that the first antenna transmits a reference carrier frequency of f_c and that the array elements have a frequency increment of Δf_o . There are K uncorrelated targets located at different ranges and angles, denoted by (r_k, θ_k) . Each target's range is constrained by maximum unambiguous range, which is determined by the formula $c/(2\Delta f)$ (where c is the speed of light). Specifically, r_k cannot exceed this value. Transmit steering vector for the k -th target is determined accordingly.

$$\mathbf{c}(\theta_k, R_k) = \mathbf{r}(r_k) \odot \mathbf{d}(\theta_k) \in \mathcal{C}^{M \times 1} \quad (4.0.2)$$

$$\mathbf{r}(r_k) = [1, e^{-j4\pi\Delta f r_k/c}, \dots, e^{-j4\pi(M-1)\Delta f r_k/c}]^T \in \mathcal{C}^{M \times 1} \quad (4.0.3)$$

$$\mathbf{d}(\theta_k) = [1, e^{j\pi \sin(\theta_k)}, \dots, e^{j\pi(M-1)\sin(\theta_k)}]^T \in \mathcal{C}^{M \times 1} \quad (4.0.4)$$

Transmit steering vector for the k -th target consists of two components: the range-dependent part \mathbf{r} , which is a function of r_k , and the angle-dependent part \mathbf{d} , which is a function of θ_k . The Hadamard product operator, denoted by \odot , is used to perform an element-wise multiplication between these two components. The transpose operator, denoted by \odot^T , is used to obtain the conjugate transpose of the resulting vector.

Let $x(t)$ is the sent signal represented as:

$$p(t) = x^T(t)\mathbf{c}(\theta_k, r_k) \quad (4.0.5)$$

$$p(t) = \mathbf{c}^T(\theta_k, r_k)x(t) \quad (4.0.6)$$

The k -th target's receiving spatial steering vector is given by the formula $\mathbf{b}(\theta_k)$.

$$\mathbf{b}(\theta_k) = [1, e^{j\pi \sin(\theta_k)}, \dots, e^{j\pi(N-1)\sin(\theta_k)}]^T \in \mathcal{C}^{M \times 1} \quad (4.0.7)$$

$$\mathbf{b}(\theta_k)x^T t \mathbf{c}(r_k, \theta_k) \quad (4.0.8)$$

$$\mathbf{b}(\theta_k)\mathbf{c}^T(r_k, \theta_k)x(t) + z(t) \quad (4.0.9)$$

$$\mathbf{b}(\theta_k)\mathbf{c}^T(r_k, \theta_k)x(t)x^T t + z(t)x^T t \quad (4.0.10)$$

where $x(t)x^T t$ is a matched filter which is orthogonality in nature and $z(t)x^T t$ is a matrix.

$$\mathbf{b}(\theta_k)\mathbf{c}^T(r_k, \theta_k)\mathbb{I} + z(t)x^T t \quad (4.0.11)$$

$$\mathbf{b}(\theta_k)\mathbf{c}^T(r_k, \theta_k)s(t) + z(t)x^T t \quad (4.0.12)$$

$$\tilde{\mathbf{b}}(\theta_k)\tilde{\mathbf{c}}^T(r_k, \theta_k)s(t) + z(t)\vec{x}^T t \quad (4.0.13)$$

$$\mathbf{b}(\theta_k) \otimes \mathbf{c}^T(r_k, \theta_k)s(t) + n(t) \quad (4.0.14)$$

The kronecker product operator, denoted by \otimes , is used in the expression for the transmitted signal $x(t)$. If the transmission waveforms meet the requirement for orthogonality, the output of the matched filters for the l -th pulse can be represented by:

$$y(t_l) = \mathbf{A}\mathbf{s}(t_l) + \mathbf{n}(t_l) \quad (4.0.15)$$

Where the combined transmit-receive array matrix is $A \in \mathcal{C}^{NM \times k}$.

$$\mathbf{A} = [\mathbf{b}(\theta_1) \otimes \mathbf{c}(r_1, \theta_1), \dots, \mathbf{b}(\theta_k) \otimes \mathbf{c}(r_k, \theta_k)] \quad (4.0.16)$$

Where $\mathbf{s}(t_l)$ is the signal vector after matched filters as shown below,

$$\mathbf{s}(\mathbf{t}_1) = [\mathbf{s}_1(t_1), \mathbf{s}_2(t_2), \dots, \mathbf{s}_k(t_k)]^T \in \mathcal{C}^{K \times 1} \quad (4.0.17)$$

$s_k(t_l)$ is the complex Gaussian random process with a mean of zero. The noise vector $\mathbf{n}(t_l)$ is obtained after passing the received signal through matched filters, and covariance matrix of $\mathbf{n}(t_l)$, which is obtained by passing the received signal through matched filters, can be represented as $\sigma^2\mathbb{I}MN$, where σ^2 denotes the variance of the noise and $\mathbb{I}MN$ denotes an identity matrix with dimensions $NM \times$

NM .

If L pulses are received, then received data is written as,

$$\mathbf{y} = \mathbf{A}\mathbf{s} + \mathbf{n} \in \mathcal{C}^{NML} \quad (4.0.18)$$

where $\mathbf{s} = [\mathbf{s}_1(t_1), \mathbf{s}_2(t_2), \dots, \mathbf{s}_k(t_k)] \in \mathcal{C}^{K \times L}$ and $\mathbf{n} = [\mathbf{n}_1(t_1), \mathbf{n}_2(t_2), \dots, \mathbf{n}_k(t_k)] \in \mathcal{C}^{NM \times L}$.

In this we applied sparse reconstruction techniques on MIMO FDA radar and MUSIC algorithm was used to find target parameter (angle). Specifically, we compare the performance of various sparse reconstruction algorithms using a scenario where the number of transmit antennas M and received antennas N are both 8, and there is only 1 uncorrelated target ($k = 1$). The frequency offset between adjacent transmit antennas is $\Delta f = 2 \times 10^3$. The carrier frequency is $f_c = 3 \times 10^9$, and the target's range is $\mathbf{r}_k = 1 \times 10^4$ with an angle of $\theta_k = -10$ degrees. The speed of light is assumed to be $c = 3 \times 10^8$ meters per second.

4.1 Applying sparse reconstruction algorithms

The sparse reconstruction algorithm NESTA was applied on FDA MIMO radar. Similarly, the application of FBMP applied on FDA MIMO radar and lastly OMP algorithm was applied too.

4.2 Applying MUSIC algorithm

The MUSIC algorithm is used for calculating the DOA of a signal source in the radar system. Here are the basic steps for applying the MUSIC algorithm:

1. First, to acquire data from the signal sources using a receiver array. The data should be sampled at a sufficiently high rate to capture the signals of interest.

2. Compute the received signal matrix: The received signal matrix is a matrix of size $N \times M$, where N is the number of receiver antennas and M is the number of samples. Each element of the matrix corresponds to the signal received at a particular receiver antenna at a particular time.
3. Compute the sample covariance matrix: The sample covariance matrix is computed as $R = XX^H$, where X is the received signal matrix and H denotes the Hermitian transpose (i.e., the conjugate transpose). Note that R is an $N \times N$ Hermitian positive semi-definite matrix.
4. Compute the eigen-decomposition of the covariance matrix: The eigen-decomposition of R yields its eigenvalues and eigenvectors. Sort the eigenvalues in descending order and select the $N - K$ largest eigenvalues, where K is the number of signal sources.
5. Compute the noise subspace: The noise subspace is spanned by the eigenvectors corresponding to the $N - K$ smallest eigenvalues of R .
6. Compute the spectrum: For each possible DOA angle, compute the MUSIC spectrum by projecting the steering vector of the signal onto the noise subspace and taking its norm squared. The DOA is estimated as the angles that correspond to the K highest peaks in the MUSIC spectrum.

4.3 Simulation Results

To assess the effectiveness of the technique for estimate in monostatic FDA-MIMO radar, numerous numerical simulations are conducted in this section. The comparison of the algorithms used on FDA MIMO radar is shown in figure 4.1. As it shows the NESTA, FBMP and OMP algorithm applied on FDA MIMO radar and shows performance of SNR Vs MSE. As SNR is increasing MSE is decreasing gradually. The NESTA method produced MSE values of 0.376 dB, 0.142 dB, 0.0207 dB, and 0.0025 dB for SNRs of 0 dB, 4 dB, 12 dB, and 20 dB, respectively. On the other hand, applying the FBMP algorithm on FDA MIMO radar resulted

in MSE values of 0.3775 dB, 0.14 dB, 0.02375 dB, and 0.0025 dB for SNRs of 0 dB, 4 dB, 12 dB, and 20 dB, respectively. Meanwhile, the OMP method yielded MSE values of 0.21 dB, 0.092 dB, 0.01625 dB, and 0.00125 dB for SNRs of 0 dB, 4 dB, 12 dB, and 20 dB, respectively.

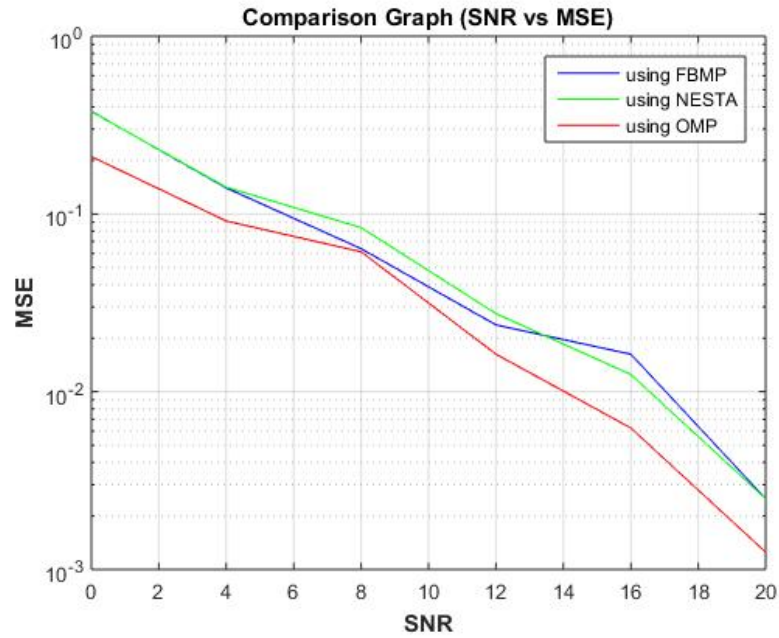


Figure 4.1: Comparison of different algorithms applied on FDA .

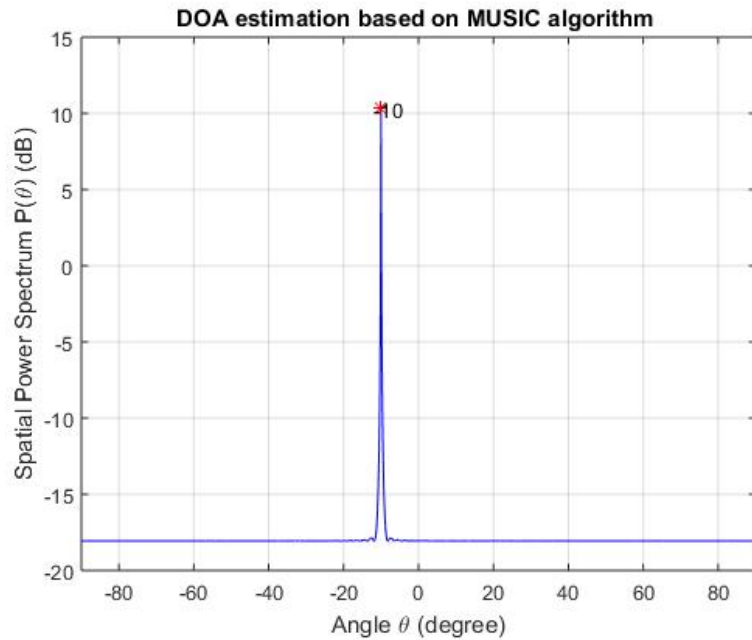


Figure 4.2: Music algorithm applied on FDA .

We use the MUSIC algorithm to simulate the Direction of Arrival estimation. The Algorithm takes transmit antennas as $M = 8$ and the receive antennas as $N = 8$ and generates the signal data accordingly. The true location of the target is also provided, and the measurement data is simulated based on this information. We then compute the covariance matrix of the measurements and perform eigenvalue decomposition. The noise subspace is obtained, and the spatial power spectrum is determined using it. Peaks of the spatial power spectrum correspond to the DOA estimates, which are plotted and displayed in Figure 4.2.

Through simulation, the performance of the different algorithms were examined and analyzed. Figures 4.3 depict the results obtained when the number of pulses is set to 100. Hence it shows that the music algorithm applied on FDA and FBMP has almost the same performance and is better than NESTA.

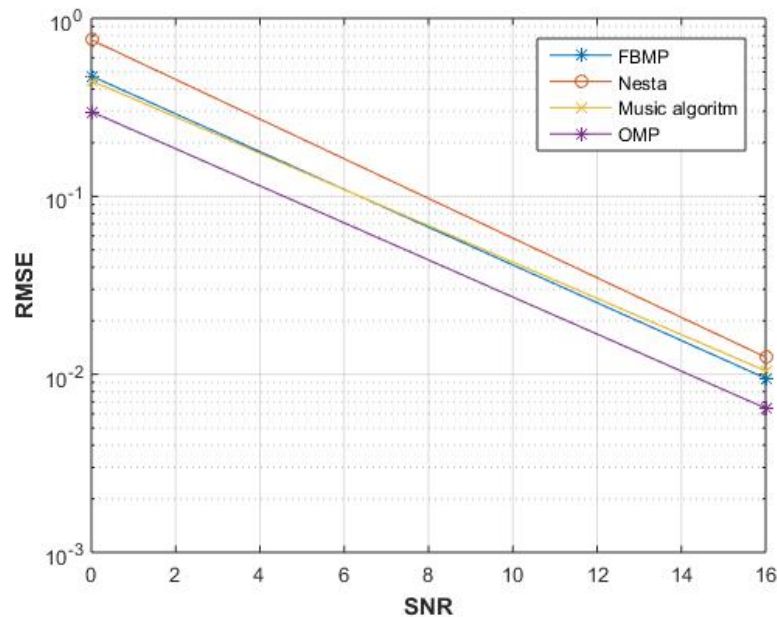


Figure 4.3: Comparison of different algorithms RMSE of angle versus SNR .

CHAPTER 5

Conclusion

In this thesis, a reduced dimension MUSIC method for monostatic FDA-MIMO radar was proposed and different sparse algorithms were applied which included NESTA, FBMP and OMP. These algorithms were applied on it and comparison was done by finding the SNR values and MSE values. The goal is to calculate Minimum Mean Squared Error and Signal to Noise Ratio estimates of the sparse vector, which are used to evaluate the accuracy of the estimation. Numerical simulations have demonstrated that the Fast Bayesian Matching Pursuit (FBMP) algorithm is a reliable approximation to the MMSE estimator, and while Orthogonal Matching Pursuit (OMP) performs slightly better than NESTA, FBMP stands out as a flexible and computationally efficient method that can be used for various sparse reconstruction problems. We also considered direction-of-arrival estimation by MUSIC algorithm. The numerical simulations validate that the suggested algorithm outperforms other algorithms in terms of angle estimation.

In the future, research in this area is likely to focus on developing more accurate and efficient algorithms for target parameter estimation using FDA radar. This may involve exploring new sparse reconstruction techniques, as well as optimizing existing algorithms to reduce computational complexity and improve accuracy. Additionally, researchers may investigate the use of deep learning algorithms for target parameter estimation in FDA radar. Deep learning has shown promise in a variety of signal processing applications, and it may be useful for developing more

CHAPTER 5: CONCLUSION

robust and accurate algorithms for target parameter estimation in FDA radar.

Overall, the future work in this area is likely to focus on developing more advanced algorithms and techniques for target parameter estimation in FDA radar, with the ultimate goal of improving radar performance in a variety of applications.

References

- [1] M. A. Richards, *Fundamentals of Radar Signal Processing*. New York: McGrawHill, 2005, pp. 1–22.
- [2] M. I. Skolnik, *Introduction to Radar Systems*, 3rd ed. New York: McGraw-Hill, 2001, pp. 1-16, 540–589.
- [3] M. I. Skolnik, “Fifty years of radar,” *Proceedings of the IEEE*, vol. 73, no. 2, pp.182–197, 1985.
- [4] W. L. Melvin and J. A. Scheer, *Principles of Modern Radar : Radar Applications, Volume 3*. Raleigh, United States: The Institution of Engineering and Technology, 2013.
- [5] P. Knee, *Sparse Representations for Radar with MATLAB Examples*. San Rafael, UNITED STATES: Morgan & Claypool Publishers, 2012.
- [6] J. D. Taylor, *Advanced Ultrawideband Radar [e-book] Signals, Targets, and Applications*. Boca Raton : Florence: Boca Raton : CRC Press LLC Florence : Taylor & Francis Group distributor, 2016.
- [7] P. Antonik, M.C. Wicks, H. D. Griffiths, C. J. Baker, “Frequency diverse array radars,” *Proceedings of the IEEE Radar*, Verona, NY, April 2006, pp.215-217.
- [8] W.Q.Wang, “Range-angle dependent transmit beampattern synthesis for linear frequency diverse arrays,” *IEEE Transaction on Antennas and Propagation* , vol.61, pp. 4073-4081, 2013.
- [9] W. Q. Wang, H. Z. Shao, “Range-angle localization of targets by a double-pulse frequency diverse array radar,” *IEEE J. Select. Topics Signal Process.*, vol. 8, pp. 106114, 2014.
- [10] W. Q. Wang, H. C. So, “Transmit sub aperturing for range and angle estimation in frequency diverse array radar,” *IEEE Trans. Signal Process.*, vol. 62, pp. 20002011, 2014.
- [11] G. Davis, S. Mallat, M. Avellaneda, *Adaptive greedy approximations*. *Constr. Approx.* 13(1), 57–98 (1997).

REFERENCES

- [12] S. Mallat, Z. Zhang, Matching pursuits with time-frequency dictionaries. *IEEE Trans. Signal Process.* 41(12), 3397–3415 (1993).
- [13] J.A. Tropp, Greed is good: algorithmic results for sparse approximation. *IEEE Trans. Inf. Theory* 50(10), 2231–2242 (2004).
- [14] J.A. Tropp, A.C. Gilbert, Signal recovery from random measurements via orthogonal matching pursuit. *IEEE Trans. Inf. Theory* 53(12), 4655–4666 (2007).
- [15] D. Needell, J.A. Tropp, CoSaMP: iterative signal recovery from noisy samples. *Appl. Comput. Harmon. Anal.* (2008). <https://doi.org/10.1016/j.acha.2008.07.002>.
- [16] D. Needell, J.A. Tropp, CoSaMP: iterative signal recovery from incomplete and inaccurate samples. *ACM Technical Report*, 2008-01 (California Institute of Technology, Pasadena, 2008).
- [17] Wang, W. Q. (2016). Overview of frequency diverse array in radar and navigation applications. *IET Radar, Sonar & Navigation*, 10(6), 1001-1012.
- [18] Khan, W., Qureshi, I. M., & Saeed, S. (2014). Frequency diverse array radar with logarithmically increasing frequency offset. *IEEE antennas and wireless propagation letters*, 14, 499-502.
- [19] Khan, W., & Qureshi, I. M. (2014). Frequency diverse array radar with time-dependent frequency offset. *IEEE Antennas and Wireless Propagation Letters*, 13, 758-761.
- [20] Wang, W. Q. (2015). Frequency diverse array antenna: New opportunities. *IEEE Antennas and Propagation Magazine*, 57(2), 145-152.
- [21] Jones, A. M., & Rigling, B. D. (2012, January). Frequency diverse array radar receiver architectures. In *2012 International Waveform Diversity & Design Conference (WDD)* (pp. 211-217). IEEE.
- [22] S. Brady and A. F. I. O. T. W.-P. A. O. S. O. ENGINEERING, “Frequency Diverse Array Radar: Signal Characterization and Measurement Accuracy,” 2010.
- [23] Baizert, P., Hale, T. B., Temple, M. A., & Wicks, M. C. (2006). Forward-looking radar GMTI benefits using a linear frequency diverse array. *Electronics Letters*, 42(22), 1311-1312.
- [24] Jones, A. M., & Rigling, B. D. (2012, May). Planar frequency diverse array receiver architecture. In *2012 IEEE Radar Conference* (pp. 0145-0150). IEEE.
- [25] Huang, L., Zong, Z., Zhang, S., & Wang, W. Q. (2021). Joint two-dimensional deception countering ISAR via frequency diverse array. *IEEE Signal Processing Letters*, 28, 773-777.

REFERENCES

- [26] Chen, T., & Xia, D. (2019, October). Joint angle and range estimation for frequency diverse array using multi-layer perceptron neural network. In 2019 IEEE 19th International Conference on Communication Technology (ICCT) (pp. 265-269). IEEE.
- [27]] Liao, Y., Wang, J., & Liu, Q. H. (2020). Transmit beam pattern synthesis for frequency diverse array with particle swarm frequency offset optimization. *IEEE Transactions on Antennas and Propagation*, 69(2), 892-901.
- [28] Xu, Y., & Xu, J. (2018). Corrections to “range-angle-dependent beamforming of pulsed-frequency diverse array” [Jul 15 3262-3267]. *IEEE Transactions on Antennas and Propagation*, 66(11), 6466-6468.
- [29] Wang, Z., & Song, Y. (2021). A waveform design method for frequency diverse array systems based on diversity linear chirp waveforms. *International Journal of Microwave and Wireless Technologies*, 13(10), 1031-1038.
- [30] Basit, A., Qureshi, I. M., Khan, W., ur Rehman, S., & Khan, M. M. (2017). Beam pattern synthesis for an FDA radar with Hamming window-based nonuniform frequency offset. *IEEE Antennas and Wireless Propagation Letters*, 16, 2283-2286.
- [31] P. F. Sammartino, C. J. Baker, and H. D. Griffiths, “Frequency diverse MIMO techniques for radar,” *IEEE Trans. Aerosp. Electron. Syst.*, vol. 49, no. 1, pp. 201–222, Jan. 2013.
- [32] T. Eker, S. Demir, and A. Hizal, “Exploitation of linear frequency modulation continuous waveform (LFMCW) for frequency diverse arrays,” *IEEE Trans. Antennas Propag.*, vol. 61, no. 7, pp. 3546–3553, Jul. 2013.
- [33] J. Shin et al., “Full-wave simulation of frequency diverse array antenna using the FDTD method,” in *Proc. Asia-Pacific Microw. Conf. Dig.*, Seoul, Korea, Nov. 5–8, 2013, pp. 1070–1072.
- [34] C. Cetinepe and S. Demir, “Multipath characteristics of frequency diverse arrays over a ground plane,” *IEEE Trans. Antennas Propag.*, vol. 62, no. 7, pp. 3567–3574, Jul. 2014.
- [35] Ge, J., Xie, J., & Wang, B. (2022). Phase characteristics of frequency diverse array radar: Phase radiation pattern, phase period, and phase centre. *IET Radar, Sonar & Navigation*, 16(5), 759-774.
- [36] Ding, Z., Xie, J., & Li, Z. (2022). Adaptive transmit beamspace optimization design based on RD-log-FDA radar. *Journal of Systems Engineering and Electronics*, 33(1), 91-96.
- [37] Xiong, J., Wang, W. Q., Chen, H., and Shao, H. (2015, December). Compressive sensing-based range and angle estimation for nested FDA radar. In 2015 Asia-Pacific Signal and Information Processing Association Annual Summit and Conference (APSIPA) (pp. 608-611). IEEE.

REFERENCES

- [38] Gui, R., Wang, W. Q., Farina, A., and So, H. C. (2021). FDA radar with doppler-spreading consideration: Mainlobe clutter suppression for blind-doppler target detection. *Signal Processing*, 179, 107773.
- [39] Chen, B., Chen, X., Huang, Y., and Guan, J. (2017). Transmit beam pattern synthesis for the FDA radar. *IEEE Antennas and Wireless Propagation Letters*, 17(1), 98-101.
- [40] Xu, J., Lan, L., Liao, G., and Zhang, Y. (2017, May). Range-angle matched receiver for coherent FDA radars. In *2017 IEEE Radar Conference (RadarConf)* (pp. 0324-0328). IEEE.
- [41] Hyder, M. M., Mahata, K., and Hasan, S. M. (2021). A new target localization method for bistatic FDA radar. *Digital Signal Processing*, 108, 102902.
- [42] Gui, R., Wang, W. Q., and Shao, H. (2018, April). General receiver design for FDA radar. In *2018 IEEE Radar Conference (RadarConf18)* (pp. 0280-0285). IEEE.
- [43] Gui, R., and Wang, W. Q. (2020, September). Adaptive Transmit Power Allocation for FDA Radar With Spectral Interference Avoidance. In *2020 IEEE Radar Conference (RadarConf20)* (pp. 1-6). IEEE.
- [44] Rogers, C. A., & Popescu, D. C. (2020). Compressed Sensing MIMO Radar System for Extended Target Detection. *IEEE Systems Journal*.
- [45] Nusenu, S. Y., and Wang, W. Q. (2018, April). Dual-function FDA MIMO radar-communications system employing costas signal waveforms. In *2018 IEEE Radar Conference (RadarConf18)* (pp. 0033-0038). IEEE.
- [46] Zhu, Y., Liu, L., Lu, Z., and Zhang, S. (2019). Target detection performance analysis of FDA-MIMO radar. *IEEE Access*, 7, 164276-164285.
- [47] Hu, Y., Deng, W., Zhang, X., and Wu, X. (2021). FDA-MIMO Radar With Long-Baseline Transmit Array Using ESPRIT. *IEEE Signal Processing Letters*, 28, 1530-1534.
- [48] Feng, M., Yang, Y., Shu, Q., and Yanga, R. (2021). An improved ESPRIT-based algorithm for monostatic FDA-MIMO radar with linear or nonlinear frequency increments. *IEEE Communications Letters*.
- [49] Feng, M., Cui, Z., Yang, Y., and Shu, Q. (2020). A reduced-dimension MUSIC algorithm for monostatic FDA-MIMO radar. *IEEE Communications Letters*, 25(4), 1279-1282.
- [50] Xiong, J., Wang, W. Q., and Gao, K. (2017). FDA-MIMO radar range-angle estimation: CRLB, MSE, and resolution analysis. *IEEE Transactions on Aerospace and Electronic Systems*, 54(1), 284-294.

REFERENCES

- [51] Liu, F., Wang, X., Huang, M., Wan, L., Wang, H., and Zhang, B. (2020). A novel unitary ESPRIT algorithm for monostatic FDA-MIMO radar. *Sensors*, 20(3), 827.
- [52] Xiong, J., Wang, W. Q., & Gao, K. (2017). FDA-MIMO radar range–angle estimation: CRLB, MSE, and resolution analysis. *IEEE Transactions on Aerospace and Electronic Systems*, 54(1), 284-294.
- [53] Lan, L. A. N., Marino, A., Aubry, A., De Maio, A., Liao, G., Xu, J., & Zhang, Y. (2020). GLRT-based adaptive target detection in FDA-MIMO radar. *IEEE Transactions on Aerospace and Electronic Systems*, 57(1), 597-613.
- [54] Li, S., Zhang, L., Liu, N., Zhang, J., & Zhao, S. (2016, October). Range-angle dependent detection for FDA-MIMO radar. In 2016 CIE International Conference
- [55] Xu, J., Wang, W. Q., Cui, C., & Gui, R. (2018, July). Joint range, angle and doppler estimation for FDA-MIMO radar. In 2018 IEEE 10th Sensor Array and Multichannel Signal Processing Workshop (SAM) (pp. 499-503). IEEE.
- [56] Cheng, J., Chen, H., Gui, R., Jia, W., & Wang, W. Q. (2020, September). Persymmetric adaptive detector for FDA-MIMO radar. In 2020 IEEE Radar Conference (RadarConf20) (pp. 1-5). IEEE.
- [57] Li, B., Bai, W., & Zheng, G. (2018). Successive ESPRIT algorithm for joint DOA-range-polarization estimation with polarization sensitive FDA-MIMO radar. *IEEE Access*, 6, 36376-36382.
- [58] Xu, J., Xu, Y., & Liao, G. (2016, June). Direct data domain based adaptive beamforming for FDA-MIMO radar. In 2016 IEEE Statistical Signal Processing Workshop (SSP) (pp. 1-5). IEEE.
- [59] Tang, W. G., Jiang, H., & Zhang, Q. (2020). Range-angle decoupling and estimation for FDA-MIMO radar via atomic norm minimization and accelerated proximal gradient. *IEEE Signal Processing Letters*, 27, 366-370.
- [60] Xiong, J., Wang, W. Q., Cui, C., & Gao, K. (2017). Cognitive FDA-MIMO radar for LPI transmit beamforming. *IET Radar, Sonar & Navigation*, 11(10), 1574-1580.
- [61] Yan, Y., Cai, J., & Wang, W. Q. (2019). Two-stage ESPRIT for unambiguous angle and range estimation in FDA-MIMO radar. *Digital Signal Processing*, 92, 151-165.
- [62] Xu, J., Liao, G., Zhu, S., Huang, L., & So, H. C. (2015). Joint range and angle estimation using MIMO radar with frequency diverse array. *IEEE Transactions on Signal Processing*, 63(13), 3396-3410.

REFERENCES

- [63] 19 Chen, X., Chen, B., Xue, Y., Chen, W., & Huang, Y. (2018, August). Space-range-Doppler focus processing: A novel solution for moving target integration and estimation using FDA-MIMO radar. In 2018 International Conference on Radar (RADAR) (pp. 1-4). IEEE.
- [64] Xu, J., Liao, G., Zhu, S., & So, H. C. (2015). Deceptive jamming suppression with frequency diverse MIMO radar. *Signal Processing*, 113, 9-17.
- [65] Yalcin, E., Ozdemir, O., & Taskin, U. (2017, December). Sparsity based regularization for microwave imaging with NESTA algorithm. In 2017 IEEE Conference on Antenna Measurements & Applications (CAMA) (pp. 282-283). IEEE.
- [66] Nam, Y., & Lee, N. (2019). Bayesian matching pursuit: A finite-alphabet sparse signal recovery algorithm for quantized compressive sensing. *IEEE Signal Processing Letters*, 26(9), 1285-1289.
- [67] Schniter, P., Potter, L. C., & Ziniel, J. (2008, January). Fast Bayesian matching pursuit. In 2008 Information Theory and Applications Workshop (pp. 326-333). IEEE.
- [68] Cai, T. T., & Wang, L. (2011). Orthogonal matching pursuit for sparse signal recovery with noise. *IEEE Transactions on Information theory*, 57(7), 4680-4688.
- [69] Karabulut, G. Z., & Yongacoglu, A. (2004, September). Sparse channel estimation using orthogonal matching pursuit algorithm. In *IEEE 60th Vehicular Technology Conference, 2004. VTC2004-Fall. 2004* (Vol. 6, pp. 3880-3884). IEEE.
- [70] Masood, M., & Al-Naffouri, T. Y. (2013). Sparse reconstruction using distribution agnostic Bayesian matching pursuit. *IEEE Transactions on Signal Processing*, 61(21), 5298-5309.
- [71] Tomioka, R., & Sugiyama, M. (2009). Dual-augmented Lagrangian method for efficient sparse reconstruction. *IEEE Signal Processing Letters*, 16(12), 1067-1070.
- [72] Shi, Z., Zhou, C., Gu, Y., Goodman, N. A., & Qu, F. (2016). Source estimation using coprime array: A sparse reconstruction perspective. *IEEE Sensors Journal*, 17(3), 755-765.
- [73] Wu, H., & Wang, S. (2012). Adaptive sparsity matching pursuit algorithm for sparse reconstruction. *IEEE Signal Processing Letters*, 19(8), 471-474.
- [74] Hu, N., Ye, Z., Xu, D., & Cao, S. (2012). A sparse recovery algorithm for DOA estimation using weighted subspace fitting. *Signal processing*, 92(10), 2566-2570.

REFERENCES

- [75] Quadeer, A. A., & Al-Naffouri, T. Y. (2012). Structure-based Bayesian sparse reconstruction. *IEEE Transactions on Signal Processing*, 60(12), 6354-6367.
- [76] Ganguly, S., Ghosh, I., Ranjan, R., Ghosh, J., Kumar, P. K., and Mukhopadhyay, M. (2019, March). "Compressive Sensing based Off-Grid DOA Estimation using OMP Algorithm". In *2019 6th International Conference on Signal Processing and Integrated Networks (SPIN)* (pp. 772-775). IEEE.

APPENDIX A

First Appendix

The separate numbering of appendices is also supported by LaTeX. The *appendix* macro can be used to indicate that following chapters are to be numbered as appendices. Only use the *appendix* macro once for all appendices.